Proc. 5th Intl Conf. On Hydrodynamics ICHD2002
Tainan, Taiwan, Oct. 31~ Nov. 2, 2002

Scaling Bubble Entrainment And Dispersion In Vertical Circular Plunging Jet Flows: Freshwater Versus Seawater

Hubert CHANSON ([1]), Shin-ichi AOKI ([2]) and Ashabul HOQUE ([2])
([1]) The University of Queensland, Department of Civil Engineering, Brisbane QLD 4072, Australia
([2]) Toyohashi University of Technology, Dept. of Architecture and Civil Engineering, Toyohashi 441-8580, Japan

Abstract
At a plunging jet, air entrainment may take place downstream of the impingement perimeter. This study investigates air entrainment and bubble dispersion at vertical circular plunging jets in freshwater, salty freshwater and seawater. The results show lesser air entrainment in seawater plunging jets for identical inflow conditions. The average pseudo-chord sizes are between 4 and 6 mm for all water solutions, although more fine bubbles were detected in seawater. It is believed that surfactants and bio-chemicals harden the induction trumpet at plunge point and diminish air entrapment at impingement in seawater.

Introduction
Air bubble entrainment at plunging jet takes place when the jet impact velocity exceeds a critical velocity (Fig. 1A). Applications of plunging jets include minerals-processing flotation cells, waste-water treatment, oxygenation of mammalian-cell bio-reactors and riverine re-oxygenation weirs (e.g. CHANSON 1997). Several researchers proposed an analogy between plunging jet flows and plunging breakers: e.g., KOGA (1982), GRIFFIN (1984), HUBBARD et al. (1987), CHANSON and LEE (1997) (Fig. 1B). Most works considered laboratory plunging breakers using freshwater and there have been suggestions that air entrainment at breaking waves in the Sea might be an entirely different process.
This study investigates scale effects affecting air entrainment and bubble dispersion at vertical circular plunging jets. Three scale models were used and detailed air-water measurements were performed systematically for identical Froude numbers with freshwater, seawater and salty freshwater.

Experimental Facilities
Experiments were conducted with vertical circular plunging jets in two flumes with five configurations (Table 1).

In Model 1, the receiving channel was 0.3 m wide, 3.6 m long and 1.8 m deep. The circular nozzle was made of aluminium with a 1/2.16 contraction ratio. In Models 2, 3, 4 and 5, the receiving flume was 0.10 m wide, 0.75 m deep and 2 m long. The nozzle was sharp-edged.

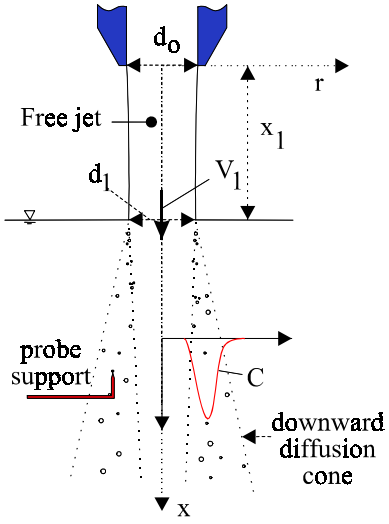

Fig. 1 - Air entrainment at plunging jets

The water discharge was measured with an orifice meter (Model 1) and with a volume per time technique in Models 2, 3, 4 and 5. Air-water flow properties were measured with single-tip

conductivity probes (needle probe design) (∅ = 0.1 & 0.35 mm). In Models 2, 4 and 5, raw probe outputs were recorded at 25 kHz for 2.6 seconds to calculate bubble chord time distributions.
Water density was measured with a Nagashima™ Standard Hydrometer GI-0361-11. Dynamic viscosity was measured with a cone and plate viscosimeter Toki™ RE80 operated at controlled temperature. Kinematic viscosity was measured with a capillary master viscosimeter Sibata™ SU-898. Surface tension was recorded using a surface wave method. Further information were reported in CHANSON et al. (2002).

Table 1 : Summary of experimental flow conditions

Mod.	d_o	x_1 ([a])	V_1	Fr_1	Comments
	m	m	m/s	m	
(1)	(2)	(3)	(4)	(5)	(6)
M1	0.025	0.1	3.5	7.2	Freshwater. Inflow pipe:
			4.1	8.4	3.5 m long, Ø=0.054 m.
			4.4	9.0	Water depth: ~1.5 m.
M2	0.0125	0.05	2.42	7.1	Freshwater. Inflow pipe:
			3.04	8.8	1.2 m long, Ø=0.0125
			3.18	9.2	m. Water depth: ~0.65
			3.46	10.0	m.
M3	0.0068	0.0273	1.79	7.1	Freshwater. Inflow pipe:
			2.16	8.5	1 m long, Ø=0.00683 m.
			2.30	9.0	Water depth: ~0.65 m.
			2.49	9.7	
M4	0.0125	0.05	2.46	7.2	Seawater. Inflow pipe:
			2.87	8.3	1.2 m long, Ø=0.0125
			3.13	9.1	m. Depth: ~0.65 m.
			3.36	9.7	
M5	0.0125	0.05	3.12	9.0	Freshwater with 34.5 ppt NaCl. Depth: 0.65m

Note : ([a]) : longitudinal distance between the nozzle and the free-surface pool.

Design procedure and physical properties
The Models were designed to be geometrically similar based upon a Froude similitude (e.g. HUGHES 1993, CHANSON 1999). The geometric scaling ratio was L_R = 2.0 between Model 1 and Models 2, 4 and 5, and L_R = 3.66 between Models 1 and 3. Similar experiments were conducted for identical Froude numbers $Fr_1 = V_1/\sqrt{g*d_1}$ where V_1 is the jet impact velocity, g is the gravity constant and d_1 is the jet diameter at impingement. Measurements were performed at similar cross-sections $(x-x_1)/r_1$ where x is the longitudinal coordinate, x_1 is the free jet length and r_1 is the jet impact radius (i.e. $r_1 = d_1/2$) (Fig. 1A).
In Models 1, 2 and 3, freshwater (tap water) was used. Water was changed after each experiment. Model 4 experiments were performed with ocean water. Seawater was collected on the Enshu coast (Pacific Ocean) off the breakers by a group of surfers. The collected waters were transparent and coarse suspended sediment material was filtered prior to the experiment. Seawater experiments were conducted within 3 days of seawater collection. Model 5 experiments were conducted with salty freshwater. The water solution was made of tap water plus 3.45% per weight of sodium chloride (NaCl) with a 99.5% quality.
Physical properties of tap water, seawater and salty freshwater were measured. The results (Table 2) are consistent with those reported by RILEY and SKIRROW (1965).

Table 2 : Measured physical properties of water

Property	Tap water	Sea water	Salty tap water	Remarks
(1)	(2)	(3)	(5)	(6)
Model(s) :	1, 2 & 3	4	5	See Table 1.
ρ (kg/m^3) :	998.2	1,024	1,024	At 20 ºC.
μ (Pa.s)	1.015 E-3	1.22 E-3	1.18 E-3	At 20 ºC.
ν (m^2/s) :	0.925 E-6	0.971 E-6	0.962 E-6	At about 22 ºC.
σ (N/m) :	0.075 0.055 ([a])	0.076	0.075	At about 22 ºC.
Conductivity (μS/cm)	87.7	49,000	53,600	At 25 ºC.
pH :	6.83	8.12	6.94	At about 22 ºC.

Notes : ρ : density; μ : dynamic viscosity; σ : surface tension between air and water; ([a]) Model 1.

Bubbly Flow Patterns

At plunging jet impact, air bubbles were entrained when the impact velocity V_1 exceeded a critical velocity V_e, called inception velocity. Although inception of air entrainment is not a precise condition (CUMMINGS and CHANSON 1999), visual observations suggested V_e = 1.58, 1.03, 0.74, 1.03 & 1.0 m/s for Models 1, 2, 3, 4 & 5 respectively and x_1/d_o = 4. The results were consistent with the observations of McKEOGH (1978) and ERVINE et al. (1980). They demonstrated also that the inception conditions were identical in freshwater, seawater and salty freshwater for an identical experiment : i.e., V_e = 1.0 m/s for d_o = 12.5 mm and x_1 = 50 mm.
For all experiments, the free jet was transparent up to impingement. For a jet velocity slightly greater than the inception velocity, individual air bubble entrainment was observed. Most entrapped bubbles were visually small (Ø < 0.5 to 1 mm). For larger jet velocities, an unstable air cavity developed at one point along the impingement perimeter. The air cavity position changed with time in an apparently random manner. Larger air packets were entrained below the air cavity with the stretching and breakup of the cavity tip. At the largest speeds, the air cavity developed all around the perimeter and most air

was entrained by elongation, stretching and breakup of the ventilated cavity. BONETTO and LAHEY (1993), CUMMINGS and CHANSON (1997) and CHANSON and BRATTBERG (1998) discussed this mechanism.

For identical experiments conducted with different water solutions, visual differences were consistently observed. In freshwater, the downward bubbly flow region was clearly defined and surrounded by rising bubbles. The flume waters appeared clear and transparent away from the plunging jet flows. Seawater experiments (Model 4) appeared to entrain more fine bubbles than freshwater plunging jets (Model 2), particularly for the largest inflow Froude numbers (i.e. $Fr_1 > 8$). Although the writers observed the entrainment of both millimetric and sub-millimetric bubbles, a large number of tiny bubbles (Ø < 0.5 mm) were seen in the entire flume. These fine bubbles were strongly affected by large recirculation eddies and their rise velocity appeared very small. In salty freshwater (Model 5), visual observations suggested a lesser presence of fine bubbles than during seawater experiments. The trend was consistent with chord time measurements, although the latter indicated a majority of millimetric bubbles for all water solutions (Table 3).

Air-Water Flow Properties

In the developing flow region, the distributions of void fraction exhibited smooth, derivative profiles (Fig. 2A). Figure 2A presents freshwater, seawater and saltwater data for an impact Froude number $Fr_1 = 9$ at two vertical locations $(x-x_1)/r_1$. In each case, the data illustrated the advective diffusion of entrained air associated with an quasi-exponential decay of the maximum air content with longitudinal distance from impingement and a broadening of the air diffusion layer. For all the experiments and jet geometry, the data were fitted by a simple analytical solution of the advective diffusion equation for air bubbles :

$$C = \frac{\frac{Q_{air}}{Q}}{4 * D^{\#} * \frac{x - x_1}{Y_{Cmax}}} * I_o\left(\frac{1}{2 * D^{\#}} * \frac{\frac{r}{Y_{Cmax}}}{\frac{x - x_1}{Y_{Cmax}}}\right) * \exp\left(-\frac{1}{4 * D^{\#}} * \frac{\left(\frac{r}{Y_{Cmax}}\right)^2 + 1}{\frac{x - x_1}{Y_{Cmax}}}\right) \quad (1)$$

where Q is the water flow rate, Q_{air} is the air flux, r is the radial distance, $D^{\#}$ is a dimensionless air bubble diffusivity, $Y_{Cmax} = r(C=C_{max})$ and I_o is the modified Bessel function of the first kind of order zero (CHANSON 1997).

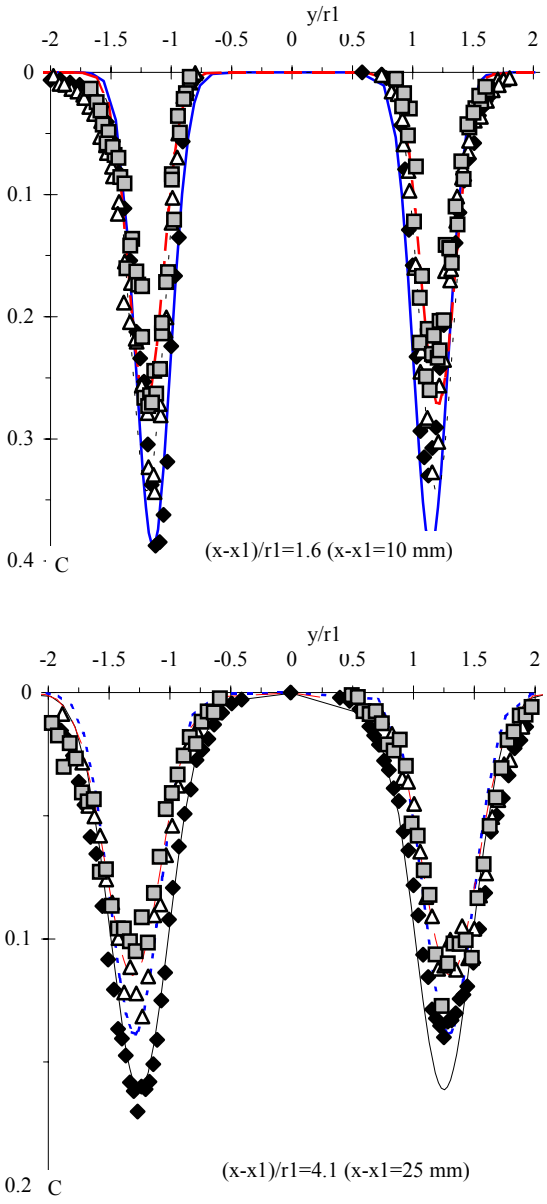

(A) Distributions of void fraction C: Model 2 (Freshwater, black diamonds), Model 4 (Seawater, grey squares), Model 5 (Salty freshwater, white triangles) - Comparison with Equation (1)

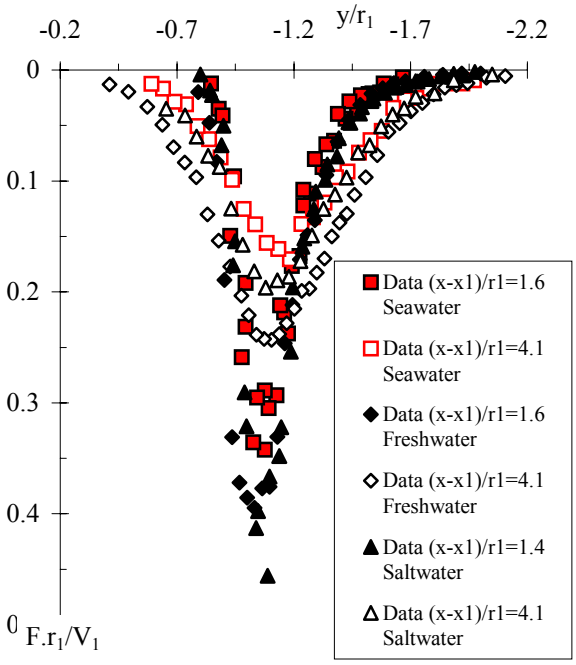

(B) Distributions of dimensionless bubble count rate $F*r_1/V_1$: Model 2 (Freshwater, Diamonds), Model 4 (Seawater, Squares), Model 5 (Salty freshwater, Triangles)

Fig. 2 - Comparison of air-water flow properties in plunging jet flows (Models 2, 4 and 5) for $Fr_1 = 9$, $d_o = 0.025$ m and $x_1/d_o = 4$

Distributions of bubble count rates were also recorded (Fig. 2B). The results highlighted maximum bubble frequency in the developing shear layers. The maximum bubble count rate occurred consistently in the inner shear region, at a radial distance smaller than $r = Y_{Cmax}$. The result was previously observed with two-dimensional jets (BRATTBERG and CHANSON 1998).

Discussion: scale effects

In freshwater plunging jets, identical results were observed between Models 1 and 2 at each cross-section for $Fr_1 = 8.4$ and 9.1. Some differences were noted for the lowest Froude number ($Fr_1 = 7$). Model 2 data showed a faster decay of void fraction and bubble count rate with increasing distance $(x-x_1)/r_1$. It is believed that the detrainment rate was greater in the small size model because the bubble rise velocity could not be scaled with a Froude similitude. For all investigated flow conditions, significantly less air was entrained in the smallest Model 3. Air entrainment was affected by significant scale effects for $We_1 < 1000$ (Model 3), where We_1 is the inflow Weber number ($We_1 = \rho*V_1^2*d_1/\sigma$).

Experiments with identical inflow conditions and different water solutions (Fig. 2) showed consistently that, for identical inflow (x_1/d_o & Fr_1), greater void factions were observed in freshwater than in seawater and saltwater. The smallest void fractions were recorded in seawater and intermediate void fractions were seen in salty freshwater. It is hypothesised that surfactants and bio-chemicals harden the induction trumpet at the plunge point and diminish air entrapment at impingement in seawater.

Bubble Chord Time Distributions

The bubble chord time t_{ch} is defined as the time spent by a bubble on the probe sensor. Chord time data were calculated from the raw signal scanned at 25 kHz at 8 locations per cross-section. The results are presented in terms of pseudo-bubble chord length ch_{ab} defined as :

$$ch_{ab} = V_1 * t_{ch} \quad (2)$$

Equation (2) predicts accurately the shape of chord size probability distribution functions and that it overestimates bubble chord lengths by about 10 to 30% (CHANSON et al. 2002).

For all water solutions and investigated inflow conditions, the data demonstrated a broad spectrum of pseudo-bubble chord lengths at each cross-section: i.e., from less than 0.5 mm to larger than 10 mm (Fig. 3). The pseudo-bubble chord length distributions were skewed with a preponderance of small bubble sizes relative to the mean. The probability of bubble chord length was the largest for bubble sizes between 0 and 2 mm. Pseudo-bubble chord length distribution results were shown in Figure 3 where the histogram columns represent the probability of chord length in 0.5 mm intervals. The last column (i.e. > 10) indicates the probability of chord lengths exceeding 10 mm. Each histogram describes all bubbles detected in a cross-section (i.e. 8 locations). Mean chord sizes and standard deviations of pseudo-chord sizes are summarised in Table 3. The results highlight that the mean pseudo-chord sizes were between 3 and 7 mm. That is, there is predominance of millimetric entrained bubbles for all water solutions, including seawater. The latter result contradicts suggestions that fine bubbles are predominantly entrained at breaking waves in the Sea.

Comparative analysis

A detailed comparison was conducted with freshwater data between Model 2 ($d_o = 12.5$ mm) and the smaller Model 3 ($d_o = 6.8$ mm). First, in the smallest model, the number of entrained bubbles with pseudo-chord size larger than 10 mm was basically negligible. The result is consistent with the observations of lesser void fraction in the smallest model for identical inflow conditions.

Second, the chord size mode was consistently smaller in the largest model (Model 2). The comparative results suggest a lesser entrainment of both large (ch_{ab} > 10 mm) and small (ch_{ab} < 1 mm) bubbles in the smallest Model 3.

Table 3 : Measured means and standard deviations of pseudo chord length ch_{ab}

Fr_1	$\frac{x-x_1}{r_1}$	Nb of bubbles	Mean ch_{ab} mm	Std ch_{ab} mm	Remarks
(1)	(2)	(3)	(4)	(5)	(6)
Model 2					Freshwater
7.07	4.19	1371	4.48	5.89	
8.81	4.11	2517	4.92	7.00	
9.20	1.64	2999	7.54	14.11	
	2.46	3341	5.79	10.78	
	4.10	2887	5.07	8.67	
9.98	4.09	3421	6.27	11.04	
Model 3					Freshwater
9.07	1.65	2058	3.83	7.78	
	2.47	1940	3.47	6.66	
	4.12	1660	3.36	5.98	
Model 4					Seawater
7.19	4.18	1198	3.08	4.58	
8.34	4.13	1947	3.90	8.31	
9.07	1.64	3787	5.56	13.40	
	2.46	3080	4.39	8.77	
	4.11	1859	4.29	8.20	
9.70	4.09	2823	4.58	9.18	
Model 5					Salty
9.04	1.64	3122	6.75	13.61	freshwater
	2.46	2561	4.50	7.56	
	4.11	2157	4.60	8.94	

Notes : Mean ch_{ab} : mean pseudo-bubble chord length; Std ch_{ab} : standard deviation of pseudo-chord length.

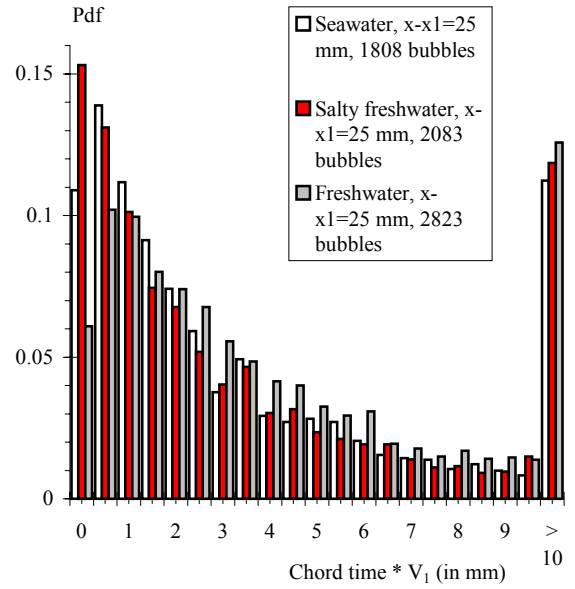

Fig. 3 - Comparison of pseudo-bubble chord sizes for x_1/d_o = 4, Fr_1 = 9 and $(x-x_1)/r_1$ = 4 between freshwater (Model 2), seawater (Model 4) and salty freshwater (Model 5)

The experimental results show consistently several trends depending upon the water solution (Fig. 3). In seawater, the typical pseudo-bubble size was millimetric with mean chord sizes of about 3 to 6 mm. In Figure 3, 75% of entrained bubbles in seawater have a pseudo-chord length greater than 1 mm. Seawater plunging jet flows contained comparatively a greater number of fine bubbles than freshwater plunging jet flows for identical inflow conditions. This is caused possibly by the combination of lesser entrainment of large-size bubbles and greater entrapment of fine bubbles (in seawater).

Pseudo-chord size distributions in seawater and saltwater were reasonably close for identical inflow conditions and cross-section locations although, in salty freshwater, the probability of bubble chord lengths appeared to be the largest for bubble sizes between 0 and 0.5 mm. A detailed analysis of probability distribution functions was conducted for pseudo-chord sizes between 0 and 2 mm with 0.1 and 0.2 mm intervals. The results showed that the difference in bubble chord size distributions was small between seawater and saltwater. The arbitrary choice of 0.5 mm intervals, as shown in Figure 3, may be misleading for small chord sizes between 0 and 1.5 mm.

Considering the size of bubbles produced by a frit, SCOTT (1975) showed that bubble coalescence was drastically reduced in saltwater compared to freshwater. BULLOCK et al. (2001) observed a similar trend in an aerated column. In the present study, the developing flow region of plunging jets was dominated by turbulent shear and momentum exchange between the jet core and the surrounding fluid, and bubble breakup was a dominant process.

Summary and Conclusion

Air entrainment and bubble dispersion at vertical circular plunging jets were investigated for a range of flow conditions and water solutions (Table 1).

Air entrainment inception conditions were nearly identical for freshwater, seawater and salty freshwater for one experiment (x_1/d_o = 4, d_o = 0.0125 m). For jet velocities greater than the onset velocity (i.e. $V_1 > V_e$), the distributions of void fraction in the developing flow region followed closely an analytical solution of the advection diffusion equation for air bubbles (i.e. Eq. (1)). In freshwater, the results highlighted some scale effects when $We_1 < 1000$ or $V_1/u_r < 10$, where V_1 is the jet impact velocity and u_r is the bubble rise velocity. For $We_1 < 1000$, the air entrainment rate was underestimated while the detrainment rate was

overestimated for $V_1/u_r < 10$.

In seawater, significantly less air was entrained than in freshwater, all inflow parameters being equal. The writers hypothesise that surfactants, biological and chemical elements harden the induction trumpet and diminish air entrapment at impingement in seawater. Air entrainment rates in saltwater were intermediate between seawater and freshwater results.

The mean pseudo-chord sizes were between 4 and 6 mm for all water solutions (Table 3). Distributions of pseudo-bubble chord sizes ranged from less than 0.5 mm to more than 10 mm. Comparatively, however, more fine bubbles were detected in seawater than in freshwater. Such fine bubbles (less than 0.5 mm) have a slower rise velocity and their underwater residence time is larger in seawater. They give a visual, misleading appearance to the air-water flow suggesting inaccurately that very fine bubbles are predominantly entrained in seawater plunging jets.

Air entrainment at plunging jets in saltwater and seawater differed : i.e., less air and smaller bubbles were entrained in seawater. The results imply that classical dimensional analysis (e.g. CHANSON 1997) is incomplete and that air entrainment at plunging jets is affected by physical, chemical and biological properties other than density, viscosity, surface tension and salinity.

Overall the study demonstrates that air entrainment in the Sea is a complicated process which cannot be modelled accurately in small-size flumes nor with fresh water experiments. It is hypothesised that living organisms in seawater might play a role in inhibiting bubble entrainment and this aspect must be investigated systematically under controlled flow conditions. Further studies of air-water plunging jet flows should also investigate air-water velocity distributions and turbulence properties.

Acknowledgements

The financial support of the Australian Academy of Science, Japan Society for the Promotion of Science and Ministry of Education, Japan is acknowledged. HC and SA thank their students and colleagues for assistance : McGIBBON, BOLDEN, IWATA, KIDA; Drs T. SUZUKI and YAMADA.

References

[1] BONETTO, F., and LAHEY, R.T. Jr (1993). "An Experimental Study on Air Carryunder due to a Plunging Liquid Jet." *Intl Jl of Multiphase Flow*, Vol. 19, No. 2, pp. 281-294. Vol. 20, No. 3, pp. 667-770.

[2] BRATTBERG, T., and CHANSON, H. (1998). "Air Entrapment and Air Bubble Dispersion at Two-Dimensional Plunging Water Jets." *Chemical Engineering Science*, Vol. 53, No. 24, pp. 4113-4127.

[3] BULLOCK, G.N., CRAWFORD, A.R., HEWSON, P.J., WALKDEN, M.J.A., and BIRD, P.A.D. (2001). "The Influence of Air and Scale on Wave Impact Pressures." *Coastal Engineering*, Vol. 42, p. 291-312.

[4] CHANSON, H. (1997). "Air Bubble Entrainment in Free-Surface Turbulent Shear Flows." *Academic Press*, London, UK, 401 pages.

[5] CHANSON, H. (1999). "The Hydraulics of Open Channel Flows : An Introduction." *Butterworth-Heinemann*, Oxford, UK, 512 pages.

[6] CHANSON, H., and LEE, J.F. (1997). "Plunging Jet Characteristics of Plunging Breakers." *Coastal Engineering*, Vol. 31, No. 1-4, July, pp. 125-141.

[7] CHANSON, H., and BRATTBERG, T. (1998). "Air Entrainment by Two-Dimensional Plunging Jets : the Impingement Region and the Very-Near Flow Field." *Proc. 1998 ASME Fluids Eng. Conf.*, FEDSM'98, Washington, USA, Paper FEDSM98-4806, 8 pages.

[8] CHANSON, H., AOKI, S., and HOQUE, A. (2002). "Similitude of Air Bubble Entrainment and Dispersion in Vertical Circular Plunging Jet Flows. An Experimental Study with Freshwater, Salty Freshwater and Seawater." *Coastal/Ocean Engineering Report*, No. COE02-1, Dept. of Architecture and Civil Eng., Toyohashi University of Technology, Japan.

[9] CUMMINGS, P.D., and CHANSON, H. (1997). "Air Entrainment in the Developing Flow Region of Plunging Jets. Part 1 Theoretical Development." *Jl of Fluids Eng.*, ASME, Vol. 119, No. 3, pp. 597-602.

[10] CUMMINGS, P.D., and CHANSON, H. (1999). "An Experimental Study of Individual Air Bubble Entrainment at a Planar Plunging Jet." *Chem. Eng. Research and Design*, Trans. IChemE, Part A, Vol. 77, No. A2, pp. 159-164

[11] GRIFFIN, O.M. (1984). "The Breaking of Ocean Surface Waves." *Naval Research Lab. Memo.*, Report No. 5337, Washington, USA.

[12] HUBBARD, D.W., GRIFFIN, O.M., and PELTZER, R.D. (1987). "Foam Generation and Air Entrainment near a Free Surface." *Naval Research Laboratory Memorandum Report 6038*, Sept., Washington, USA.

[13] HUGHES, S.A. (1993). "Physical Models and Laboratory Techniques in Coastal Engineering." *Advanced Series on Ocean Eng.*, Vol. 7, World Scientific Publ., Singapore.

[14] KOGA, M. (1982). "Bubble Entrainment in Breaking Wind Waves." *Tellus*, Vol. 34, No. 5, pp. 481-489.

[15] McKEOGH, E.J. (1978). "A Study of Air Entrainment using Plunging Water Jets." *Ph.D. thesis*, Queen's University of Belfast, UK, 374 pages.

[16] RILEY, J.P., and SKIRROW, G. (1965). "Chemical Oceanography." *Academic Press*, London, UK.

[17] SCOTT, J.C. (1975). "The preparation of Water for Surface Clean Fluid Mechanics." *Jl of Fluid Mech.*, Vol. 69, part 2, pp. 339-351.